Domains of Practical Stability near $L_{4,5}$ in the 3D Restricted Three-Body Problem

(work in progress)

Carles Simó[(1)], Priscilla Sousa-Silva[(1)] and Maisa Terra[(2)]

[(1)] Departament de Matemàtica Aplicada i Anàlisi, UB, Barcelona, Catalunya

[(2)] Departamento de Matemática, Instituto Tecnológico de Aeronáutica, São José dos Campos, SP, Brazil

carles@maia.ub.es, priandss@maia.ub.es, maisa@ita.br

International Conference
Dynamical Systems: 100 tears after Poincaré
Gijón, Asturias, 120907

The problem

We consider the 3D RTBP. It is known that for small mass ratios ($\mu < \mu_1$) the Lagrangian triangular points are **linearly stable**.

For the 2D case **nonlinear stability** is proved except for a coupled of values μ_2, μ_3.

For the 2D case **practical stability** (i.e., a big part of the dynamics occurs in tori of maximal dimension and the diffusion between them is rather slow) is proved on a domain of non-negligible measure for most of the $\mu \in (0, \mu_1)$.

Numerical evidence gives an indication that the domain of **practical stability is large**. Furthermore, in some part the **boundaries of the domain are sharp**.

This calls for **an explanation**.

In real life we can ask, for instance: **Why there exist Trojans so far from the L_4, L_5 points of the Sun-Jupiter system?**

Some preliminary information

- **3 D.O.F. Hamiltonian**
  - Particle P_3 of negligible mass moving under the gravitational influence of P_1 and P_2 of masses m_1 and m_2. Called **primaries** or **primary and secondary**.
  - The primaries describe **circular coplanar orbits** around the barycentre of P_1-P_2 and are fixed in the synodic reference frame (which rotates w.r.t. an inertial frame).
  - **Non-dimensional variables**: distance between the primaries, the sum of their masses and their angular velocity around the barycentre are normalized to one.
  - $\mu = m_2/(m_1 + m_2)$, $m_1 > m_2$ is the only parameter of the model.
- **Equations of Motion**:

$$\ddot{x} - 2\dot{y} = \Omega_x, \quad \ddot{y} + 2\dot{x} = \Omega_y, \quad \ddot{z} = \Omega_z,$$

$$\Omega(x, y, z) = \frac{1}{2}(x^2 + y^2) + \frac{1-\mu}{r_1} + \frac{\mu}{r_2} + \frac{\mu(1-\mu)}{2},$$

$$r_1 = \sqrt{(x-\mu)^2 + y^2 + z^2}, \quad r_2 = \sqrt{(x+1-\mu)^2 + y^2 + z^2}.$$

- **Integral of motion**

$$J(x, y, z, \dot{x}, \dot{y}, \dot{z}) = 2\Omega(x, y, z) - (\dot{x}^2 + \dot{y}^2 + \dot{z}^2) = C,$$

C being denoted as **Jacobi constant**.

- The 5D **energy manifold**: $\mathcal{M}(\mu, C) = \left\{(x, y, z, \dot{x}, \dot{y}, \dot{z}) \in \mathbb{R}^6 | J(x, y, z, \dot{x}, \dot{y}, \dot{z}) = C\right\}$.
- **Hill regions**:
  - Projection of $\mathcal{M}$ onto the configuration space;
  - Areas accessible to the trajectories for each C;
  - Bounded by the Zero Velocity Surfaces (ZVS).
- **Collinear equilibrium points**: $L_{1,2,3}$, on the x-axis
  - centre-centre-saddle
  - 4D central manifold: vertical and horizontal Lyapunov orbits, Halo orbits, invariant tori, other periodic orbits, chaotic regions.
- **Triangular equilibrium points**: $L_{4,5}$, at $x = \mu - \frac{1}{2}, y = \mp\frac{\sqrt{3}}{2}, z = 0$
  - Planar case: **nonlinear stability** for $\mu \in (0, \mu_1) \setminus \{\mu_2, \mu_3\}$, where for μ_j the ratio of frequencies $\left[(1 \pm (1 - 27\mu(1 - \mu))^{1/2})/2\right]^{1/2}$ is j.
    $\mu_1 = \frac{(9-\sqrt{69})}{18}$, $\mu_2 = \frac{(45-\sqrt{1833})}{90}$, $\mu_3 = \frac{(15-\sqrt{213})}{30}$.
  - Spatial case: **nonlinear stability**, in a small vicinity of the point, for $\mu \in (0, \mu_1) \setminus \{\mu_2, \mu_3\}$, except on a set of small Lebesgue measure for a fixed μ.

Some references

- Markeev, A.P., *On the stability of the triangular libration points in the circular bounded three-body problem*, Applied Math. Mech. **33** (1969), 105-110.
- Markeev, A.P., *Stability of the triangular Lagrangian solutions of the restricted three-body problem in the three-dimensional circular case*, Soviet Astronomy **15** (1972), 682-686.
- Leontovich, A.M., *On the stability of the Lagrange periodic solutions of the restricted problem of three bodies*, Soviet Math. Dokl., **3** (1962), 425-428.
- Deprit, A. and Deprit-Bartholomé, A., *Stability of the triangular Lagrangian points*, The Astronomical Journal **72**, (1967), 173-179.

Some old numerics in the planar case (both E-M)

Rough investigation (480 time units). (McKenzie, R. and Szebehely, V., *Nonlinear stability motion around the triangular libration points*, Celestial Mechanics **23** (1981), 223-229).

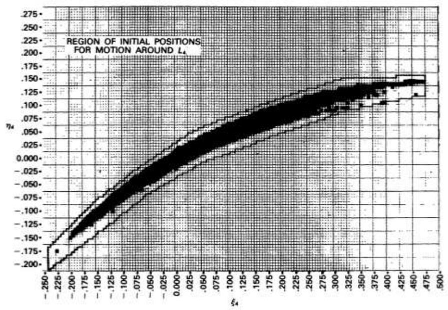

Fig. 3. Region of initial positions for motion around L_4.

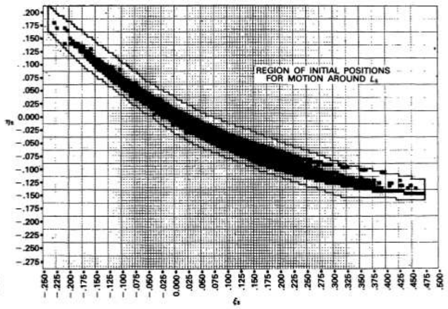

Fig. 4. Region of initial positions for motion around L_5.

Numerical evidence that the **boundary** of the stable domain is **related to the central manifold of L_3**. (Gómez, G., Jorba, A., Masdemont, J. and Simó., C., *Study of Poincaré Maps for Orbits near Lagrangian Points.* ESA Technical Report, 1993).

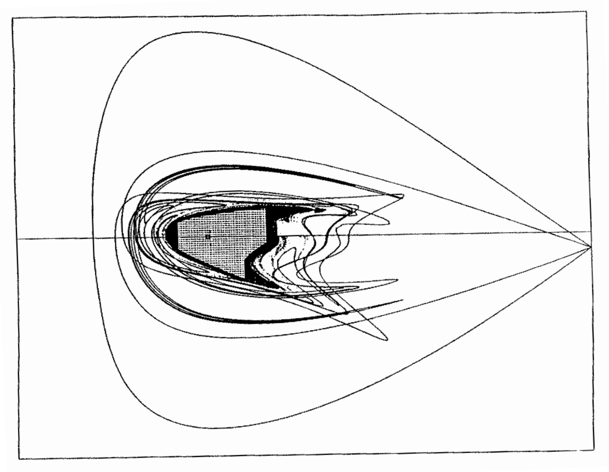

Some previous results in the 3D case

For different reasons many computations are done with **initial conditions on the ZVS** using (z, α, ρ) **as parameters** for a fixed μ:

$$x = \mu + (1+\rho)\cos(2\pi\alpha), \quad y = (1+\rho)\sin(2\pi\alpha), \quad z = z_0 \geq 0, \quad \alpha \in (0, 1/2), \quad \dot{x} = \dot{y} = \dot{z} = 0.$$

As for $\mu = 0$ one must be in $1-1$ **resonance** it is convenient to look, starting at the ZVS for values of $(z, R = 1+\rho)$ related by

$$z = \left[4(1+R^2)^{-2} - R^2\right]^{1/2} \quad \text{or} \quad \psi = 1 - \frac{1}{2}w + \frac{3}{2^5}w^2 - \frac{1}{2^8}w^3 - \frac{25}{2^{13}}w^4 + \frac{33}{2^{16}}w^5 + \mathcal{O}(w^6),$$

where $w = z^2$, $\psi = \psi(z) = R^2$. This suggests to plot $(\alpha,\ \gamma = 1 + \rho - \sqrt{\psi(z)},\ z)$. It is clear that L_5 corresponds to $\rho = 0, \alpha = 1/3, z = 0$. By symmetry, similar results are obtained for L_4.

Reasons to start at the ZVS:

- Most of the i.c. non-leading to escape are on **3D tori**. Hence, we scan a **set of positive measure** in the full phase space (not fixing C).
- The results obtained can be used as **a seed** to obtain the **relevant objects** either starting at the ZVS or not.

Anyway, the case with $IC \notin ZVS$ will be also considered later.

First we look for some results at the **quasi-boundary escape/confinement**.

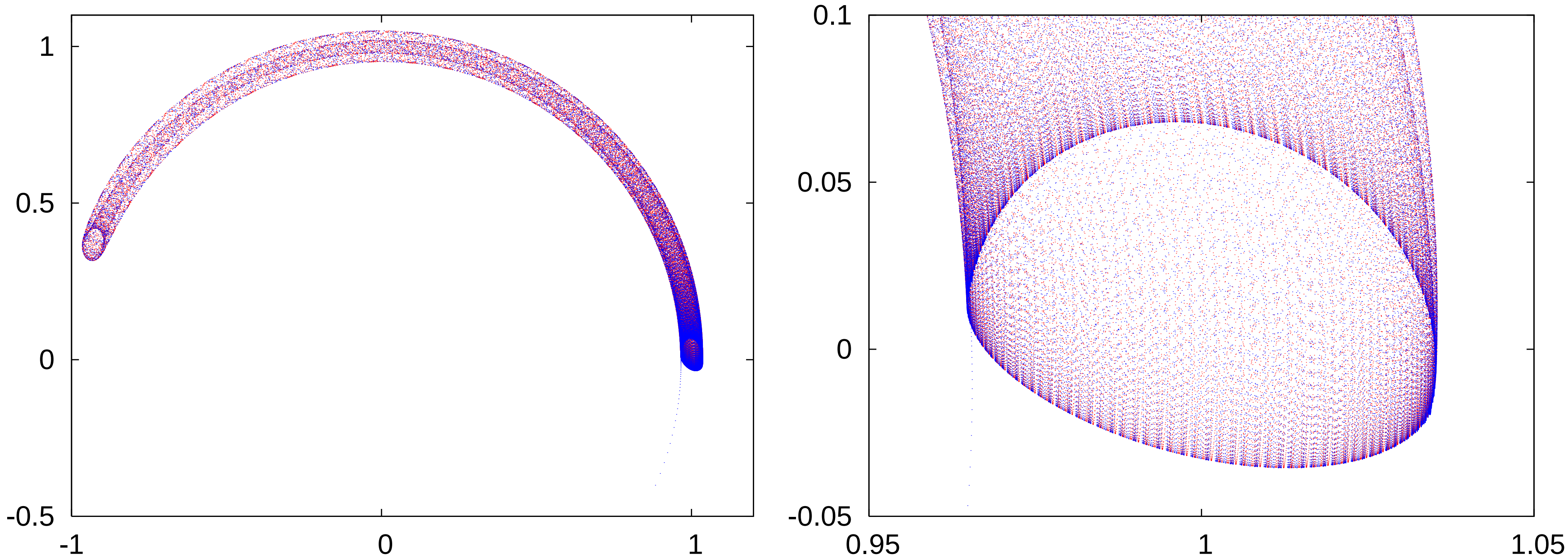

Example of a transition for $\mu = 0.0001$, $\alpha = 0.05$, $z = 0.3$. The two tori (**confined, escaping**) have ρ which differ in 10^{-10} Shown: the projections on (x, y) of the Poincaré section through $z = 0$. The **separating unstable 2D torus (or invariant curve in the section) belongs to** $W^{u,s}_{L_3}$.

In the next figure a similar plot for $\alpha = 0.4$, $z = 0.6$. Now the **separating unstable 2D torus is not in** $W^{u,s}_{L_3}$.

Our main goal is to clarify how these objects at the "boundary" are organised.

Top: initial part of Poincaré iterates and the **separating unstable invariant curve** projected on (x, y). Bottom: same curve projected on $(x, \dot{z})$ and the **2D separating unstable torus** in (x, y, z) projection.

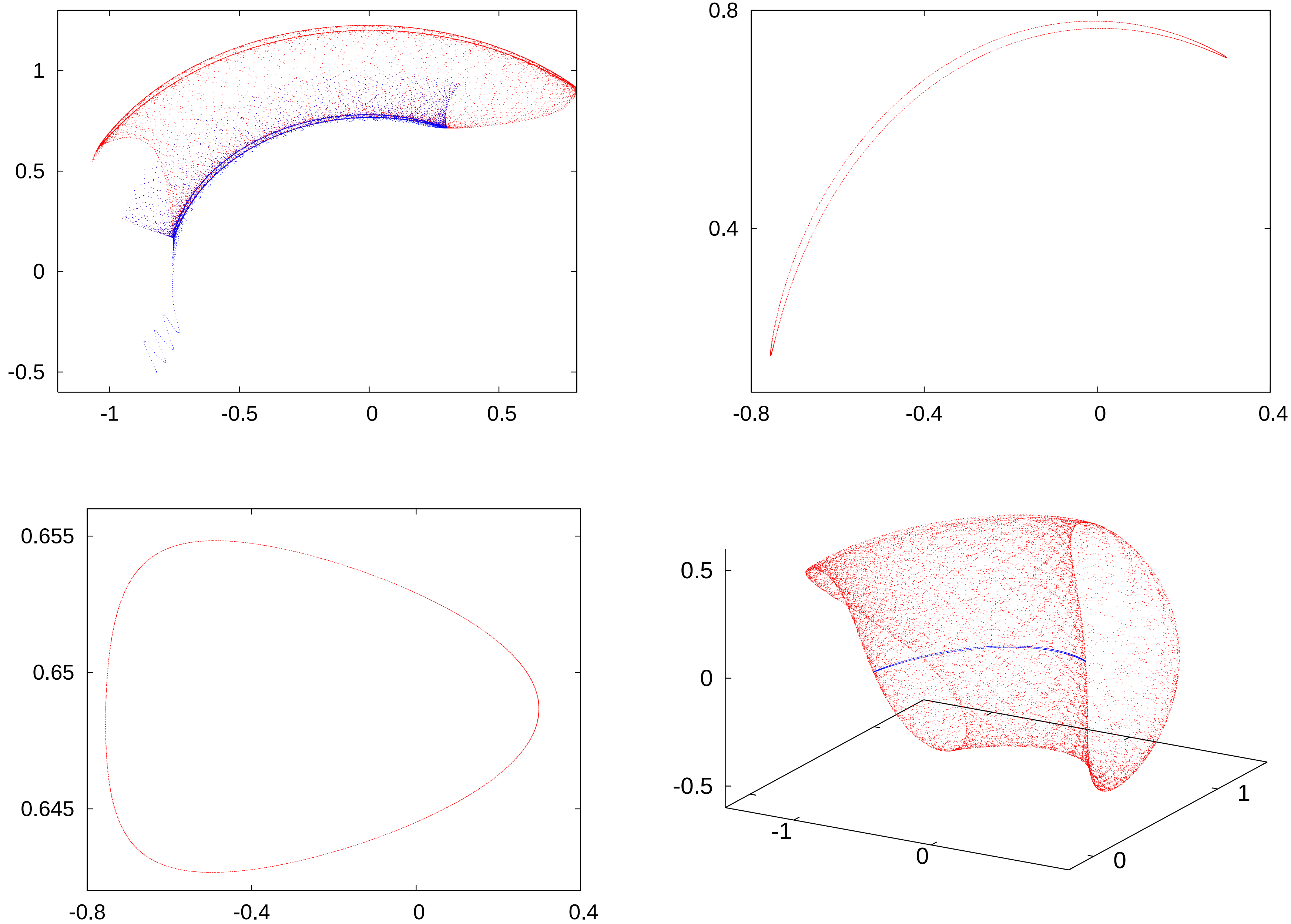

Slices of non-escaping points for $\mu = 0.001$

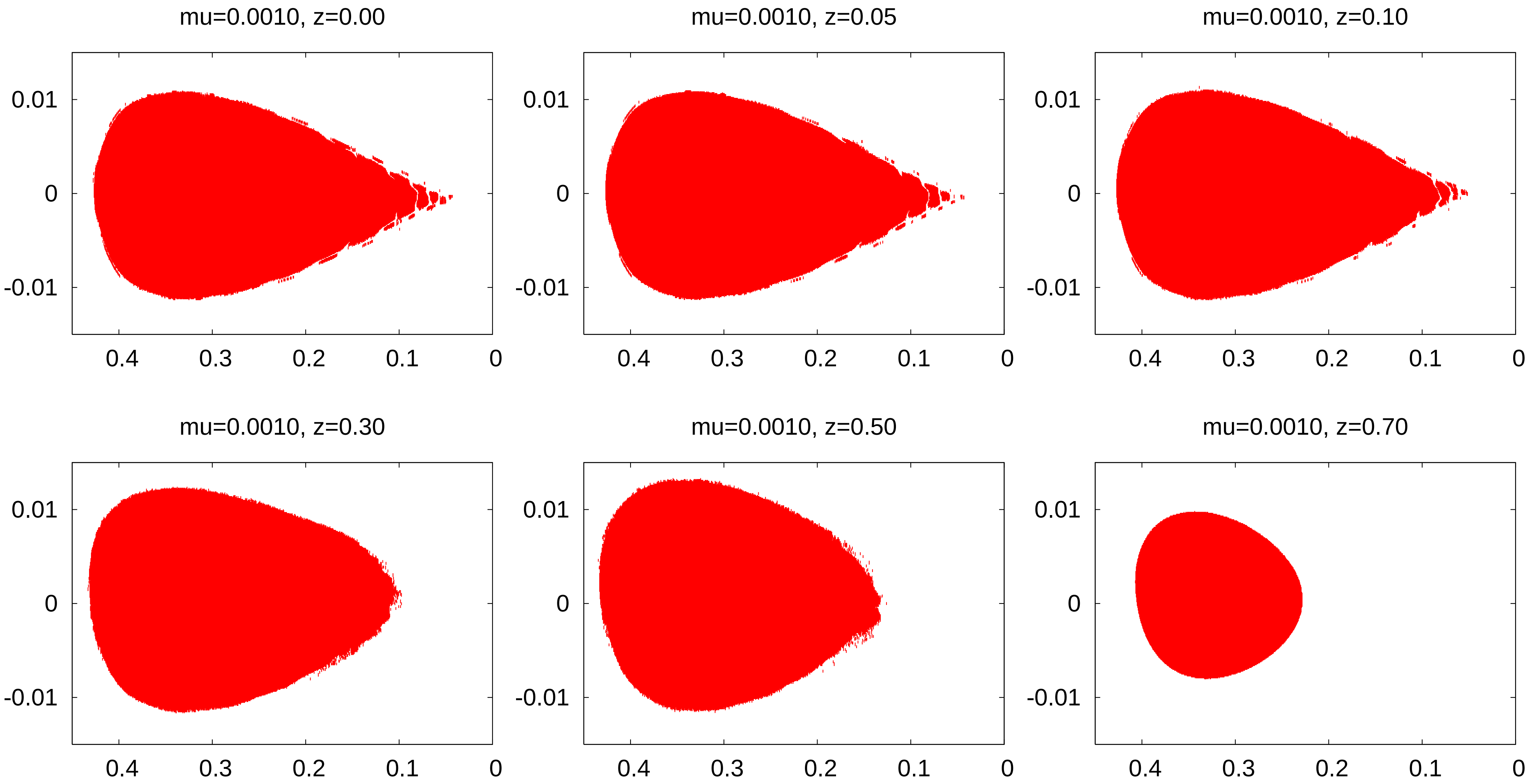

Next we show some **3D views of the "boundaries"** (inner, outer) for ρ as a function (z, α). The results are **shown in** (α, γ, z).
See `www.maia.ub.es/dsg/2006/ number 2`.

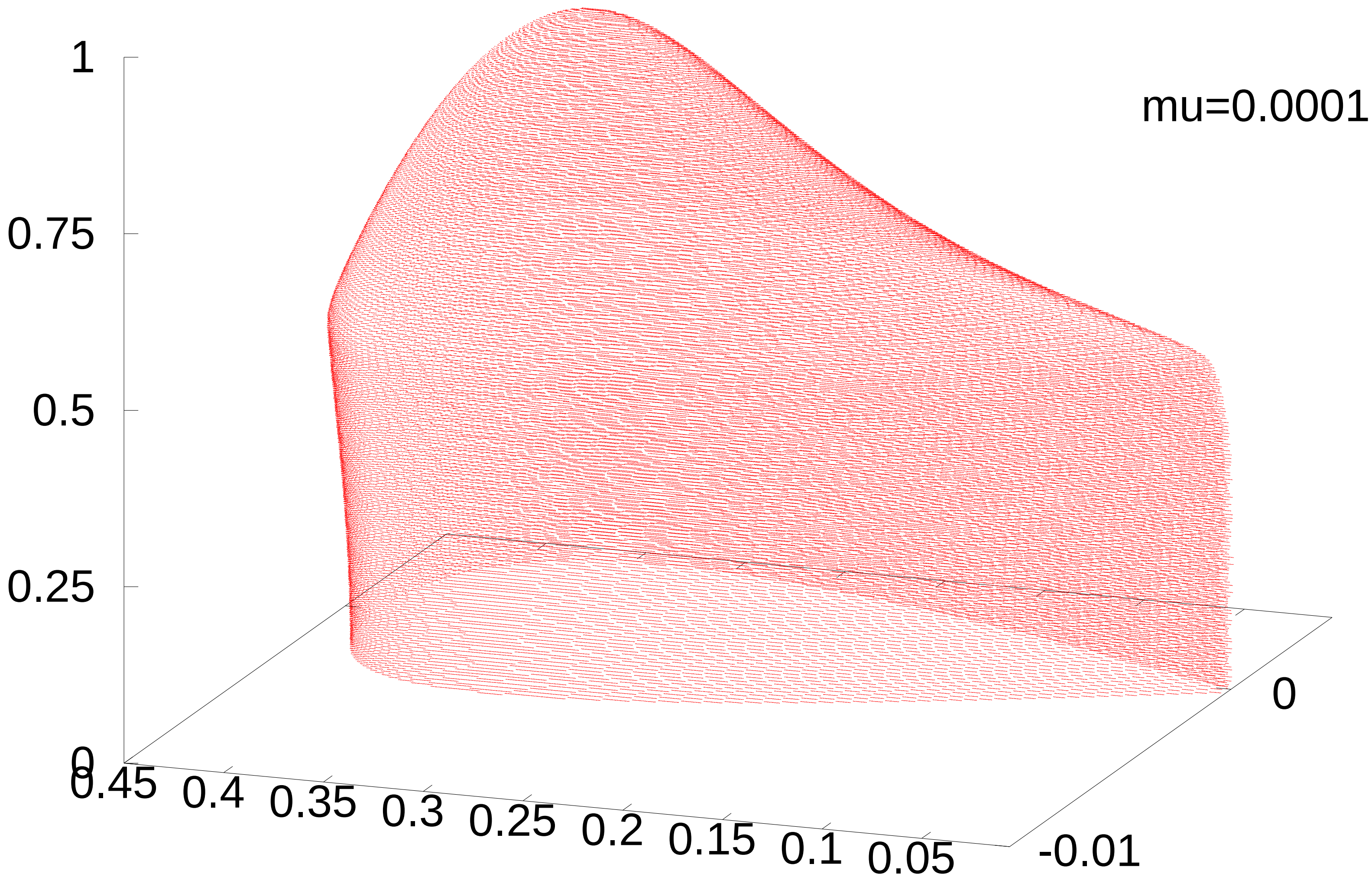

Note the **sharp change** on the behaviour of the boundary between $z = 0.4$ and $z = 0.5$.

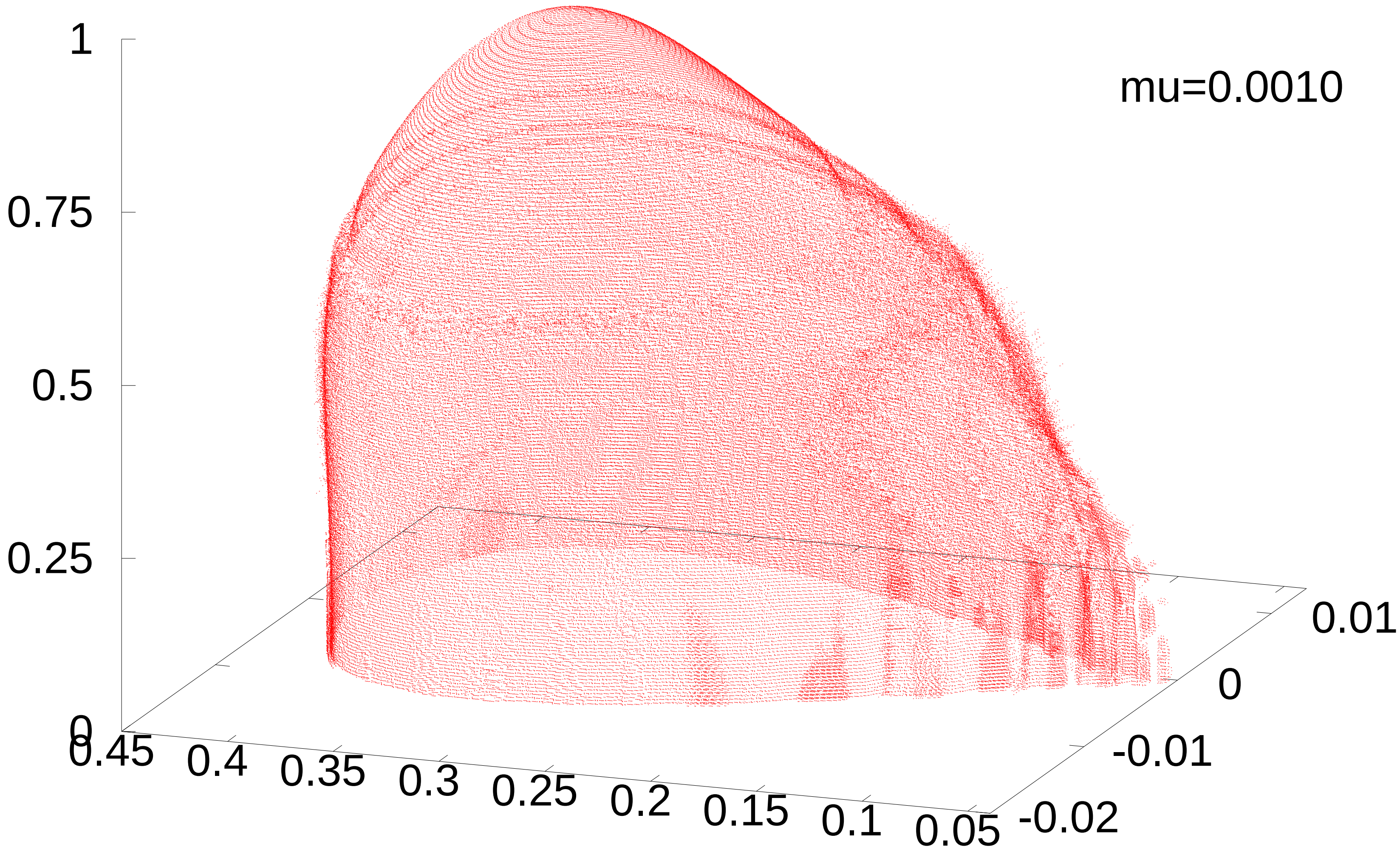

Beyond the previous change some **island-like structures** appear for small z. The value of μ is close to the **Sun-Jupiter** case.

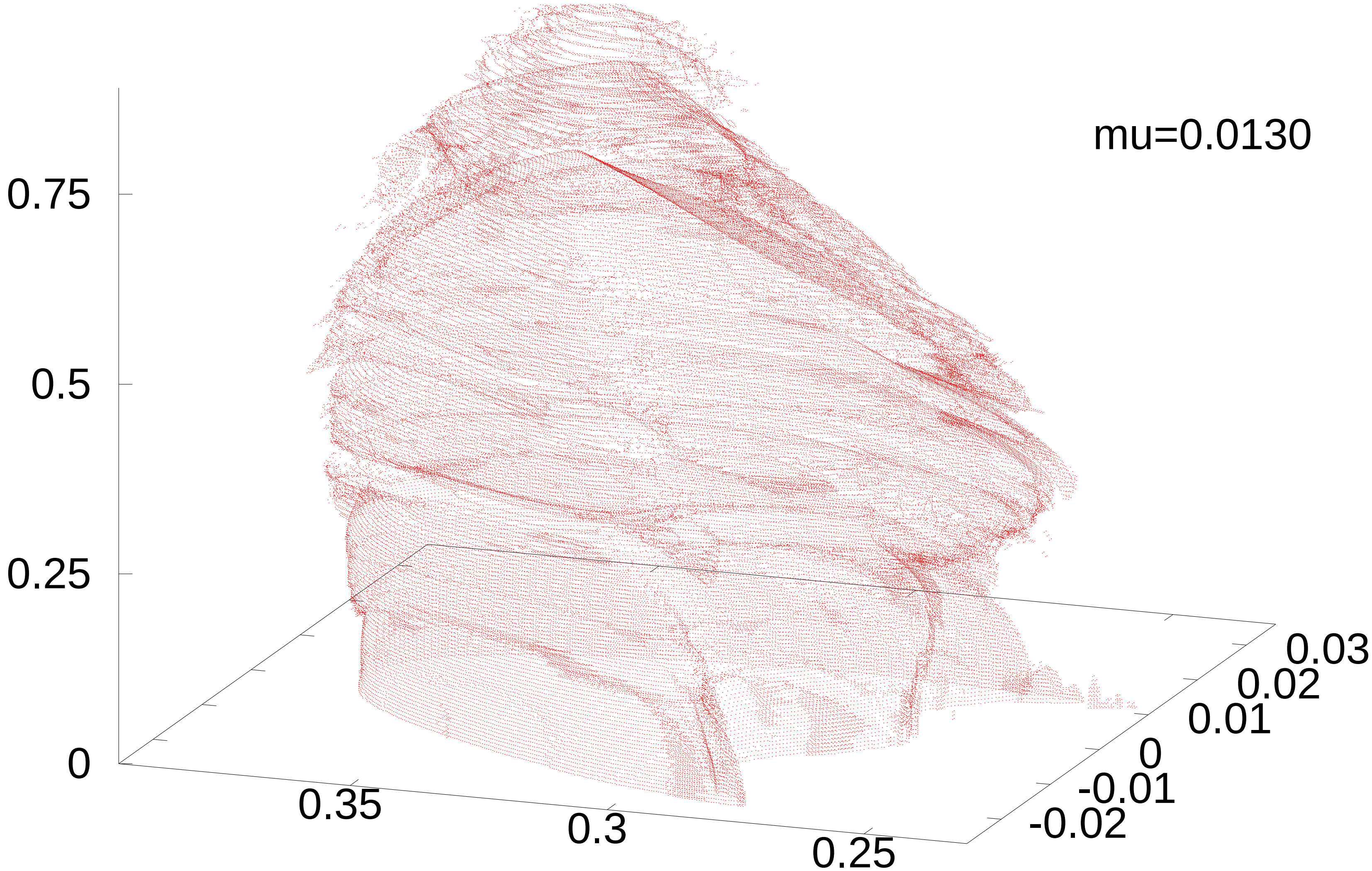

The value of μ is slightly **larger than the Earth-Moon case** and a little **below the 3 to 1 resonance at μ_3**. More **complex structures** show up.

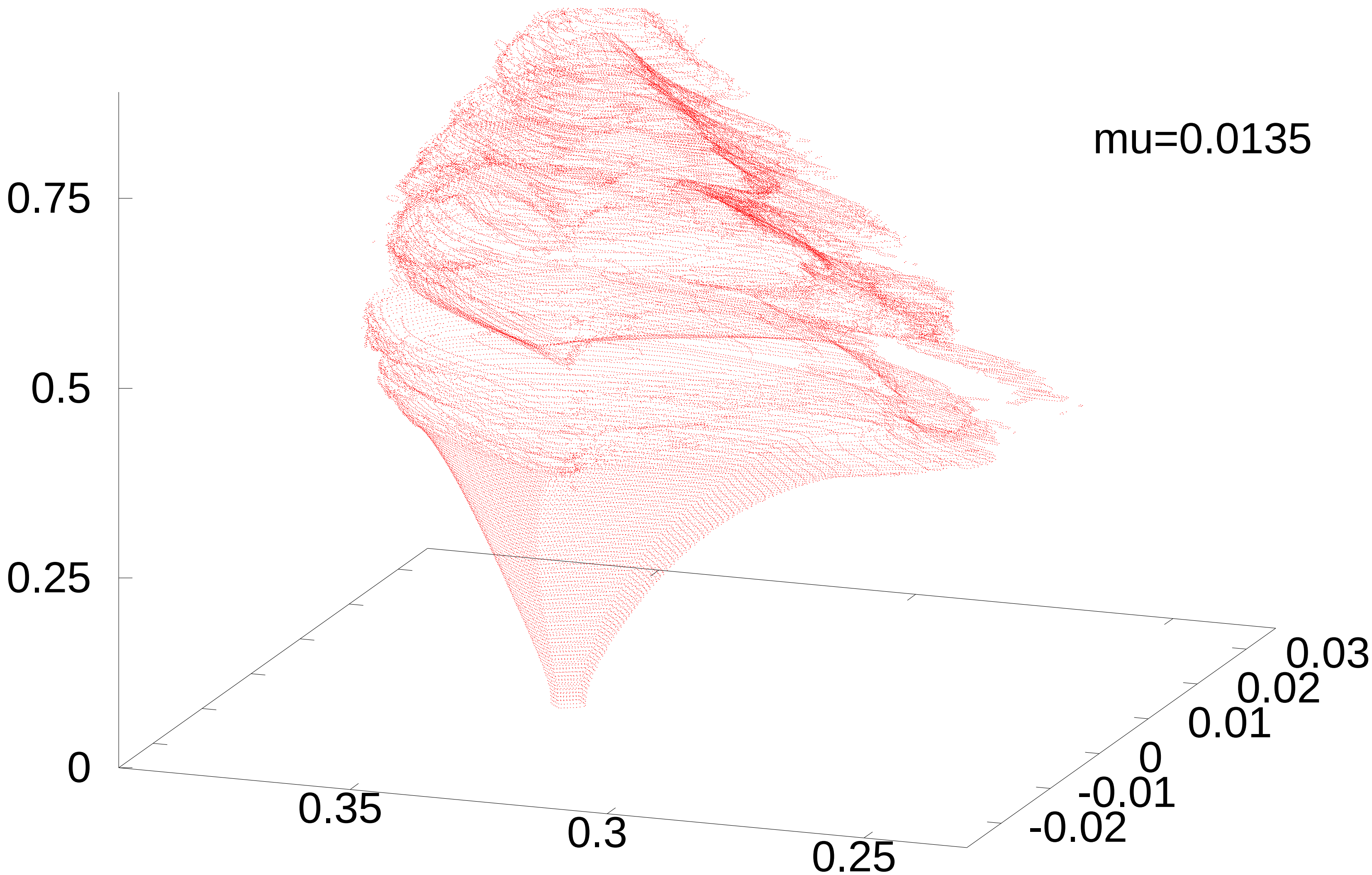

Results for $\mu = 0.0135 < \mu_3 = 0.0135160160\ldots$. Note that the stability domain is **quite small for the 2D problem, but large for the 3D one**.

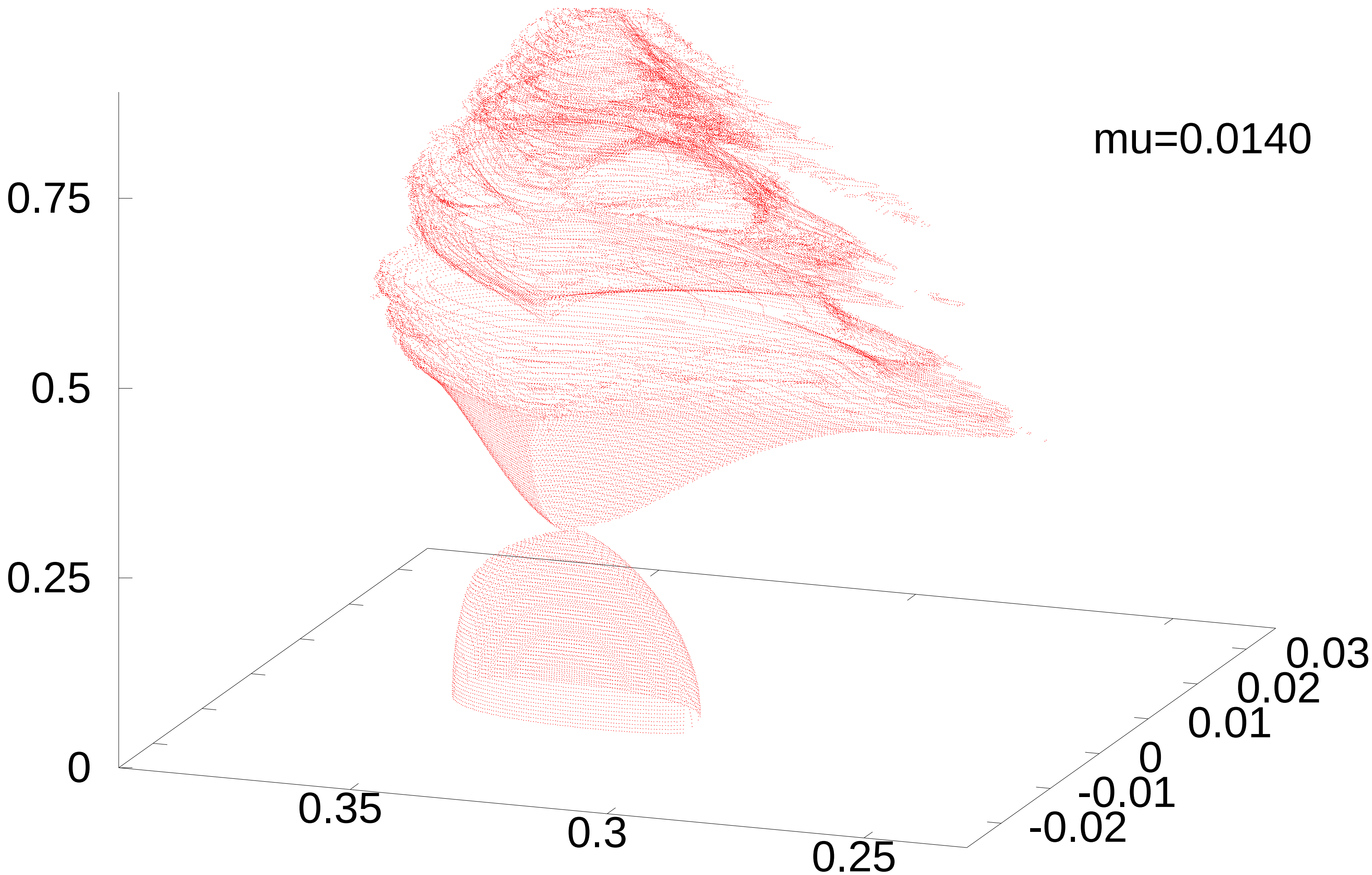

A value **slightly larger that μ_3**. Note how the stability **seems to shrink to one point** for initial conditions on the ZVS.

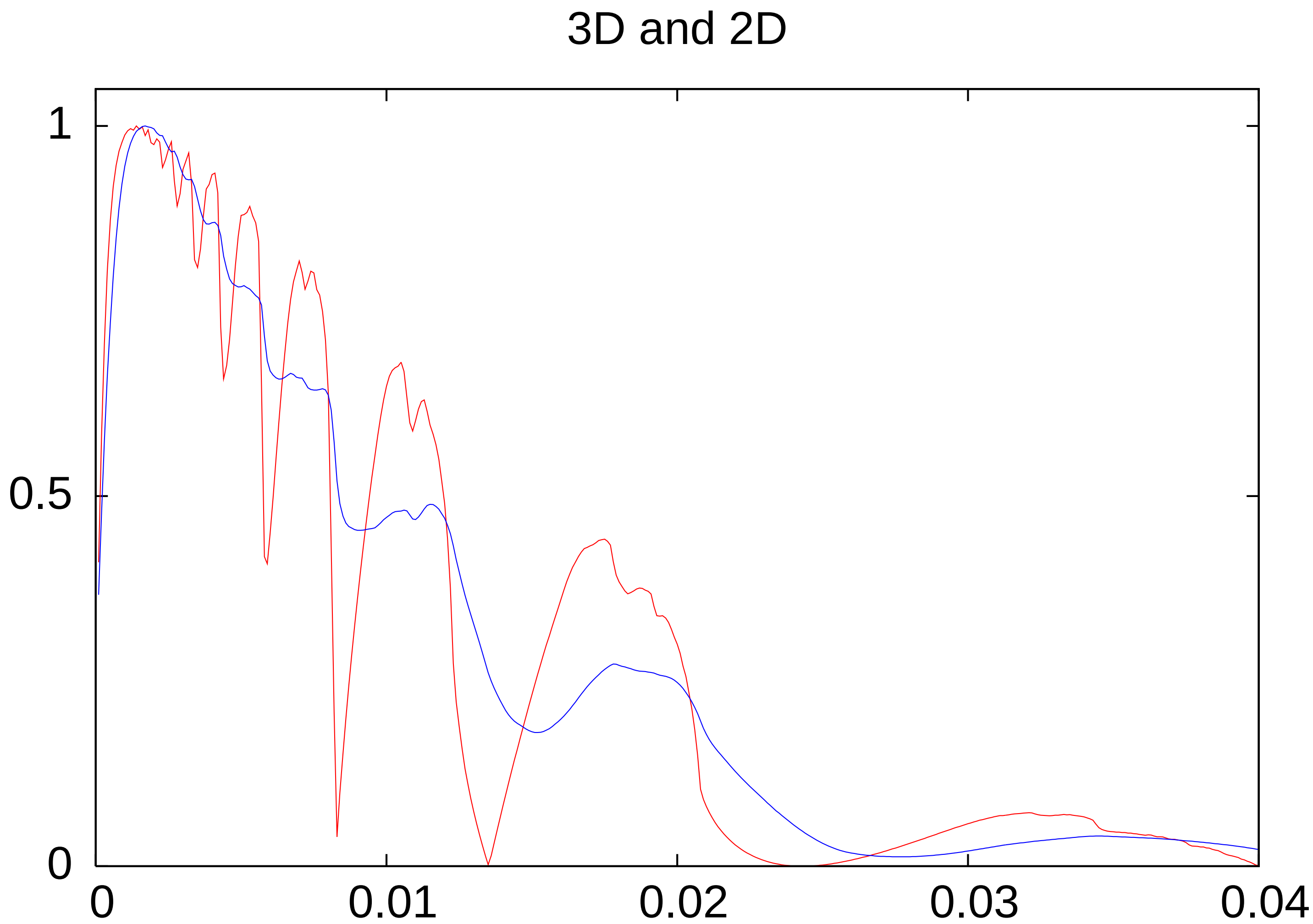

Statistics as a function of μ starting at the ZVS. Normalized **subsisting** points.
Planar case (red): 10^5 secondary revolutions, $\Delta\rho = 10^{-4}$, $\Delta\alpha = 2 \times 10^{-4}$. **Maximal value, for $\mu = 0.0014$**, 282757 points. Note the sharp change at **resonances**.
Spatial case (blue): 10^3 secondary revolutions, $\Delta\rho = 10^{-4}$, $\Delta\alpha = 5\times10^{-4}$, $\Delta z = 5\times10^{-3}$. **Maximal value, for $\mu = 0.0017$**, 19014882 points. **Milder and delayed effect of the resonances**.
In both cases **some stability subsists even for $\mu > \mu_1$** (of course).

The problem of the "practical boundaries" of stability

The standing problem: **where are the "practical boundaries" located and to which objects are related?**
Comments of this type of problem:
A "typical" result in analysis: $\exists\,\varepsilon_0 > 0$ such that if $|\varepsilon| < \varepsilon_0$ then something holds.
As an example take **KAM** theorem: for given diophantine conditions **DC** (c, τ) and a given **torsion** T, if $|\varepsilon| < \varepsilon_0$ then the torus subsist. But

- For fixed DC, **how do we determine a sharp $\varepsilon_0(T)$?**
- What can we expect for the **dynamics if $|\varepsilon| > \varepsilon_0(T)$?**
- How does ε_0 depend **on both T and the DC?**

These questions are a **challenge for the near (?) future**.

The choice of the mass parameter for research in detail

The value $\mu = 0.0002$ **has been selected**. Reasons:

- Being μ small, the boundaries are **sharper**.
- Also **possible to obtain some information by perturbation**,
- Close to the **Titan-Saturn mass ratio**.

Problem: The **escape is relatively slow**. Integration time is **large**.

Approximating the boundaries of the domain

Methodology

First: Define some **escape criterion** (e.g., (x, y) projection in some wedge near negative y axis, too close or too far from primary, too close to secondary),

Second: **scan a set of initial conditions for short time** (e.g. $10^4 \times 2\pi$, using some grid with small steps $\Delta\alpha, \Delta\rho, \delta z$). **Keep the i.c. non leading to escape**.

Third: **Repeat for longer time** for the "pixels" at a **distance less than d pixel units** from the ones which already escaped. Repeat 1 or 2 times for **longer and longer integration time** (e.g. 50000, 250000, 10^6 primary revolutions).

Fourth: Eventually do **additional refinements of ρ** for fixed α, z.

Next we display a few sections for **constant z** and for **constant α**.

We display also some results using the **paraboloid-like correction** on the ρ variable.

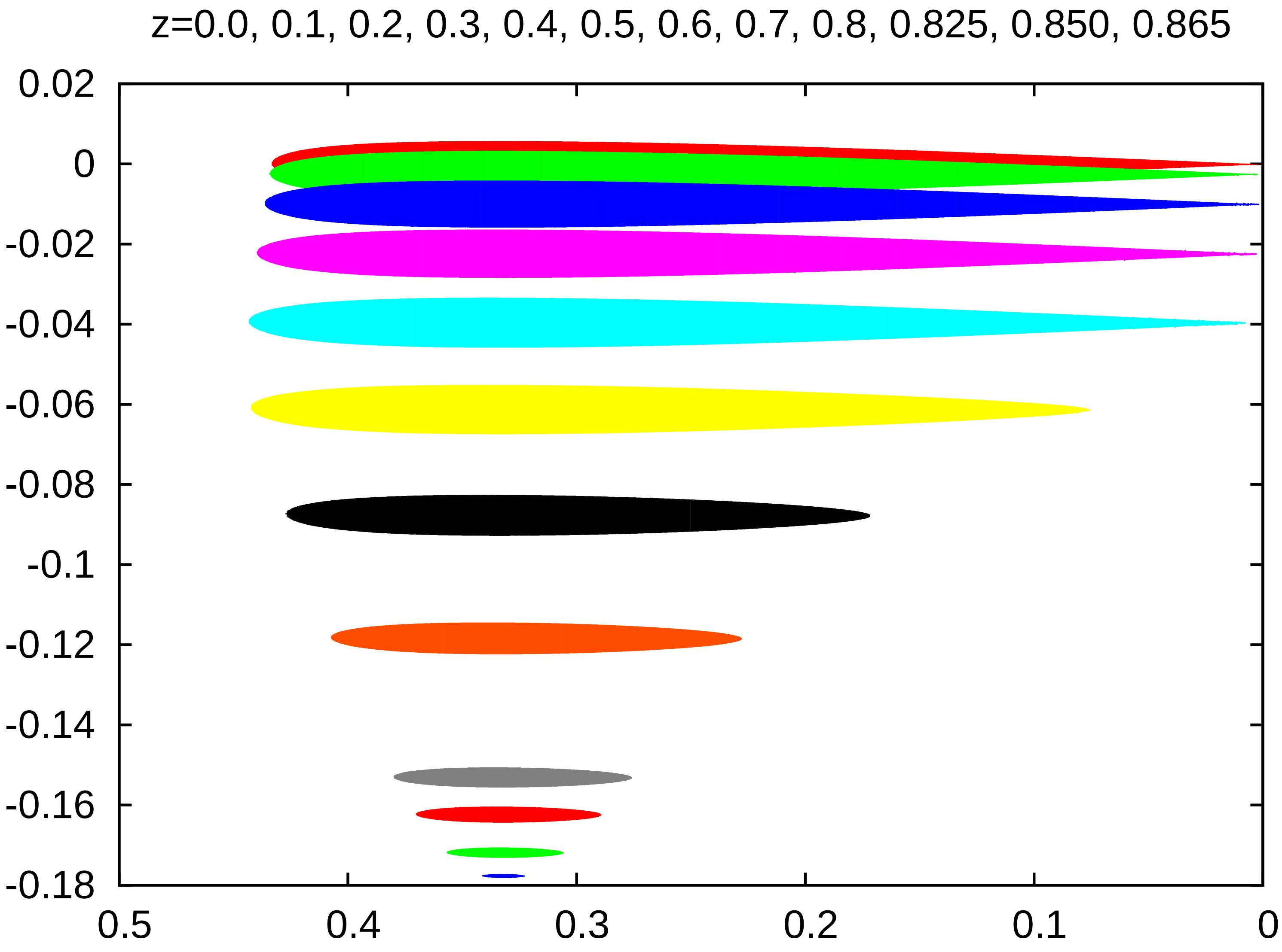

Subsisting points starting at the ZVS for different z values. Coordinates: (α, ρ)

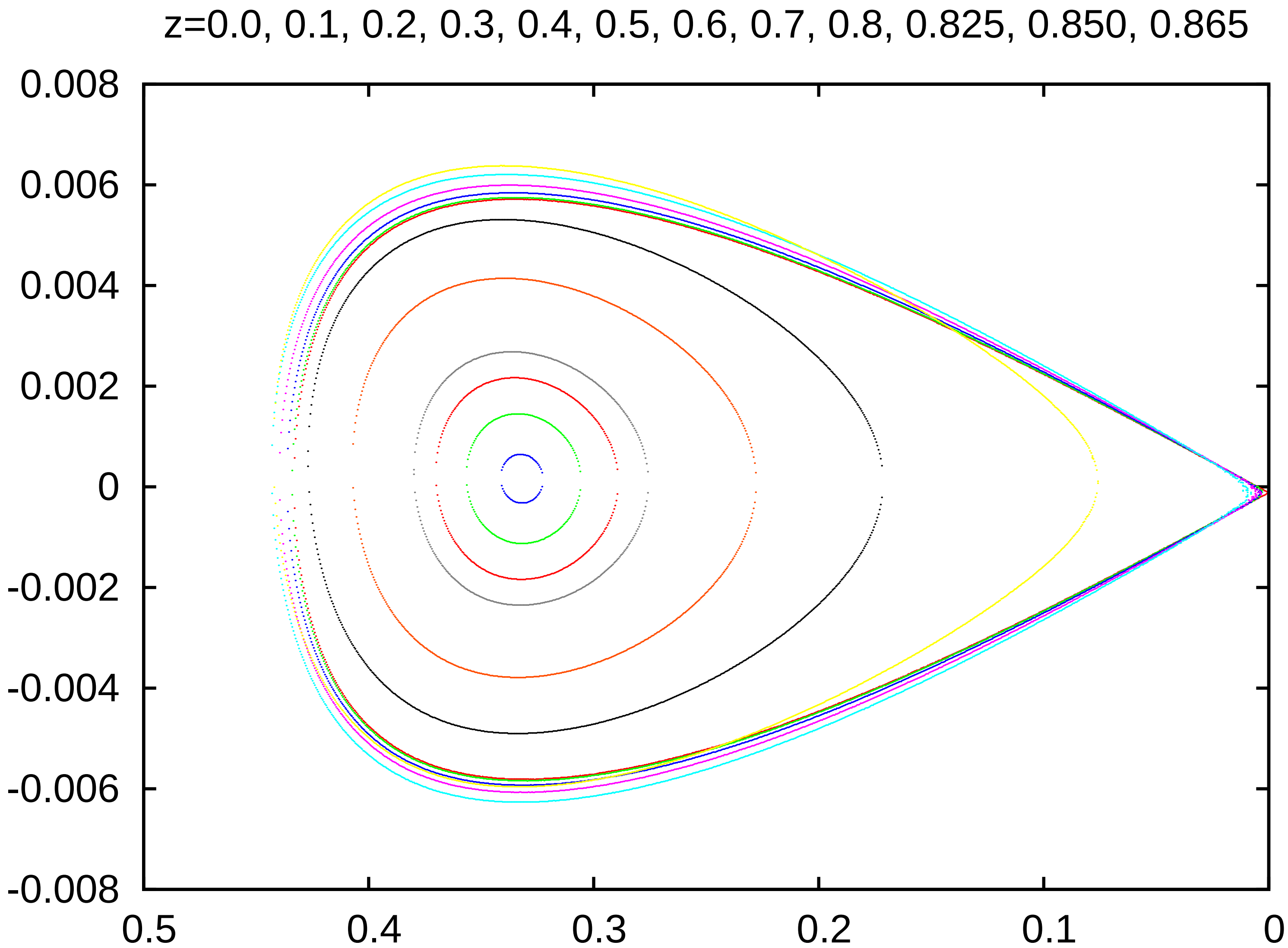

Boundaries of the previous domains for different z values, after making the **paraboloid-like** correction for ρ.

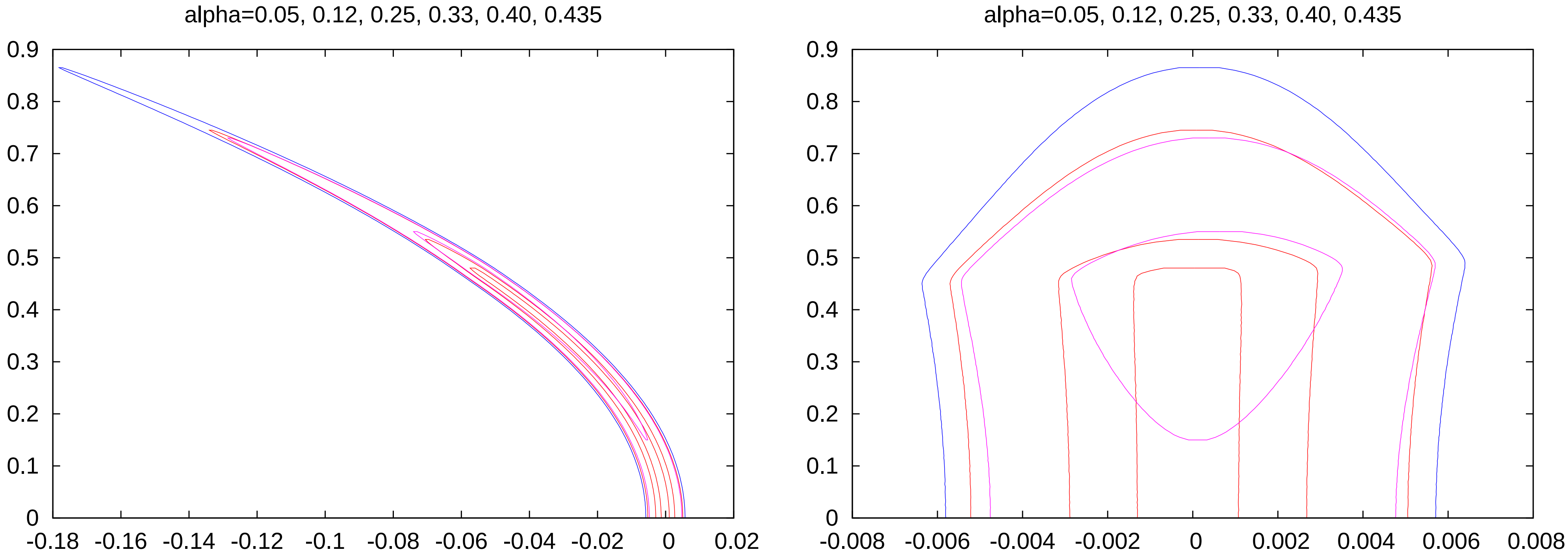

Some **sections of the boundary** starting at the ZVS for different α values. Left: in (ρ, z) variables. Right: using the **corrected ρ** instead of ρ.
Red: $\alpha = 0.05, 0.12, 0.25$. Blue: $\alpha = 0.33$; Magenta: $\alpha = 0.40, 0.435$.

Some Poincaré sections

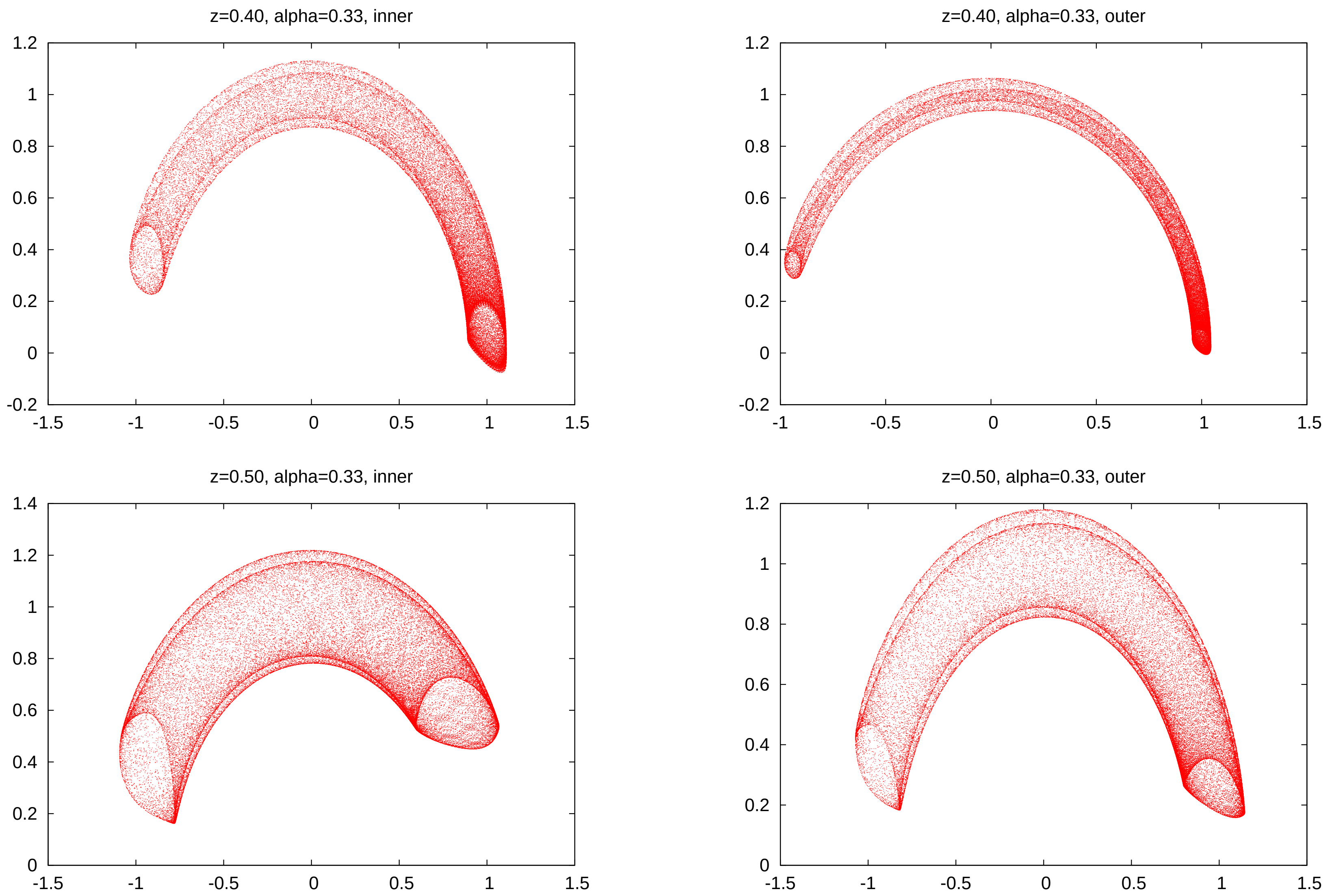

Some **Poincaré sections through** $z = 0$, $\dot{z} > 0$. Top: $z = 0.4$, $\alpha = 0.33$. Bottom: $z = 0.5$, $\alpha = 0.33$.

Some two-sections

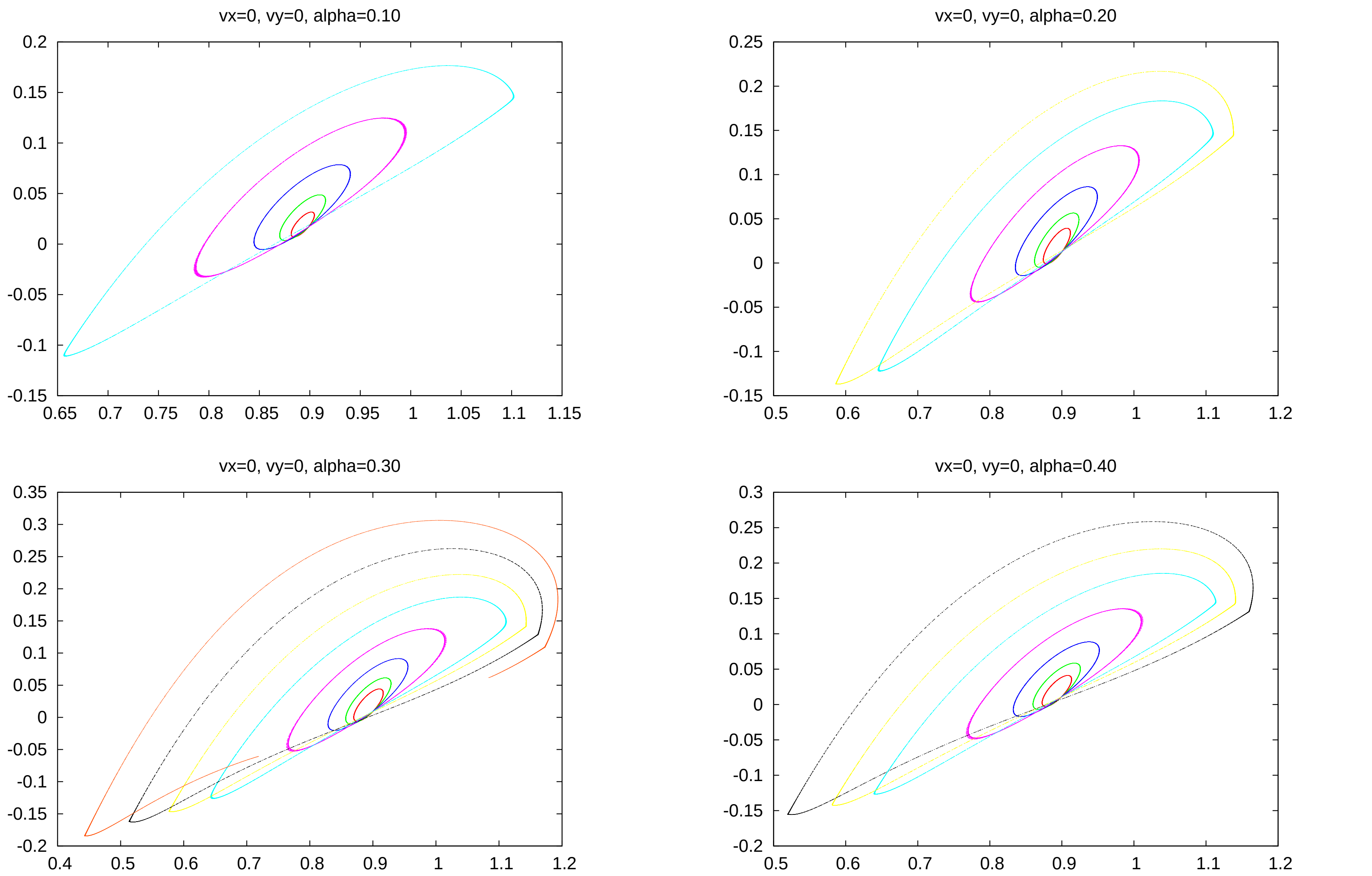

Some **two-sections**, that is, intersections of the Poincaré section with $x = x_0 (= -0.5)$ for $\alpha = 0.1,\ 0.2,\ 0.3,\ 0.4$ and different $z\ (= 0.1,\ 0.2,\ 0.3, \ldots)$.

Note the different behavior for $z \geq z_0$, $0.4 < z_0 < 0.5$.

NHIM: 2D tori

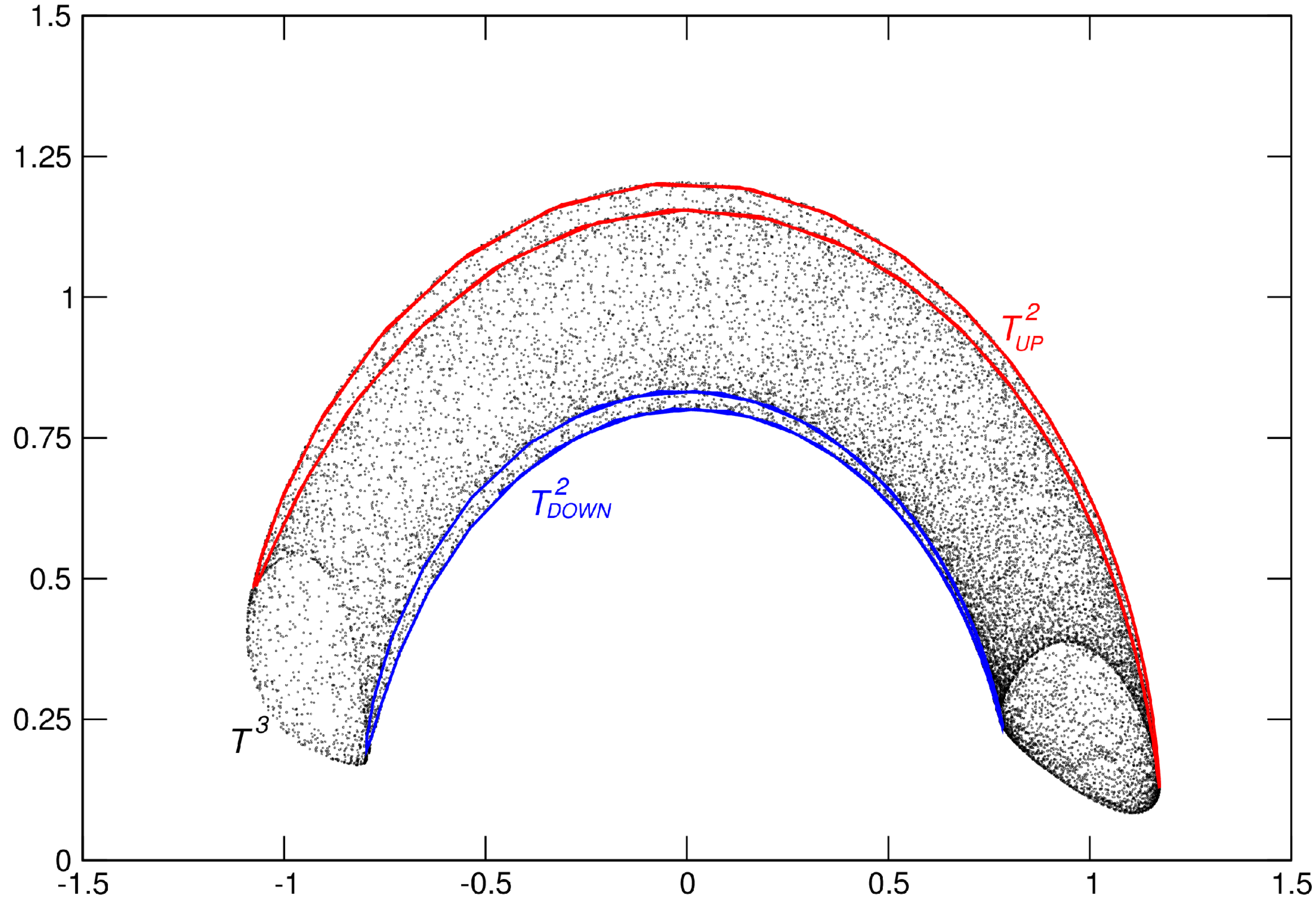

Poincaré section through $z = 0$. Initial data: $z_0 = 0.46$, $\alpha = 0.35$, inner boundary. The **approximate 2D NHIM at the boundary** are enhanced, seen as **invariant curves on the Poincaré section**.

These approximate invariant curves are **refined by standard Fourier methods**.

Continuation: vs rotation number and vs Jacobi constant

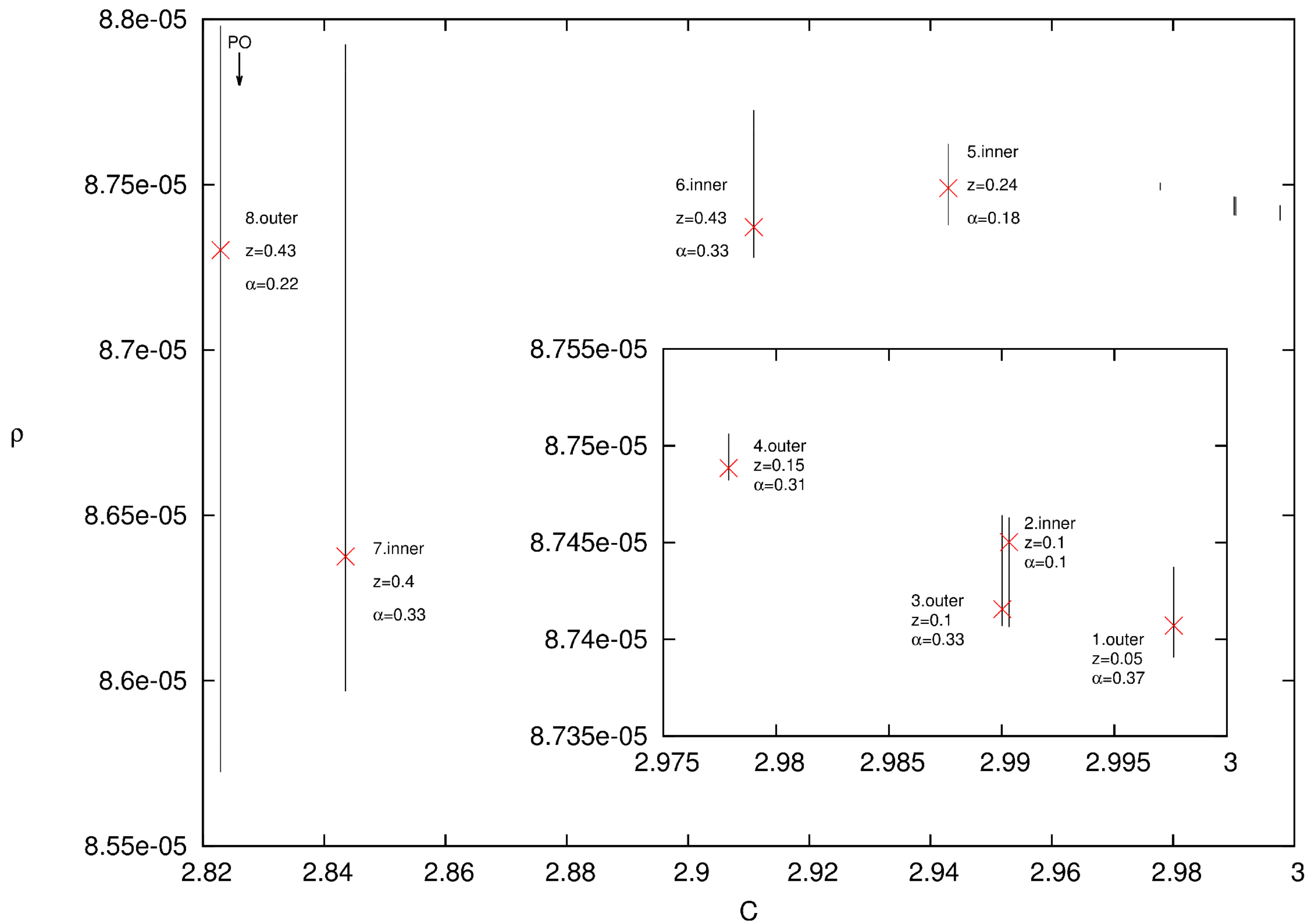

When a NH invariant curve is available on the Poincaré section $z = 0$ it is **continued**, either **wrt C for fixed rotation number** (chosen to be a rational multiple of golden mean) or **along fixed C** (with rotation numbers taken as before). The **invariant curves are also identified by the data on the ZVS**, in that plot with small z_0. Note the **small value of the rotation number** (due to the small horizontal frequency at L_3).

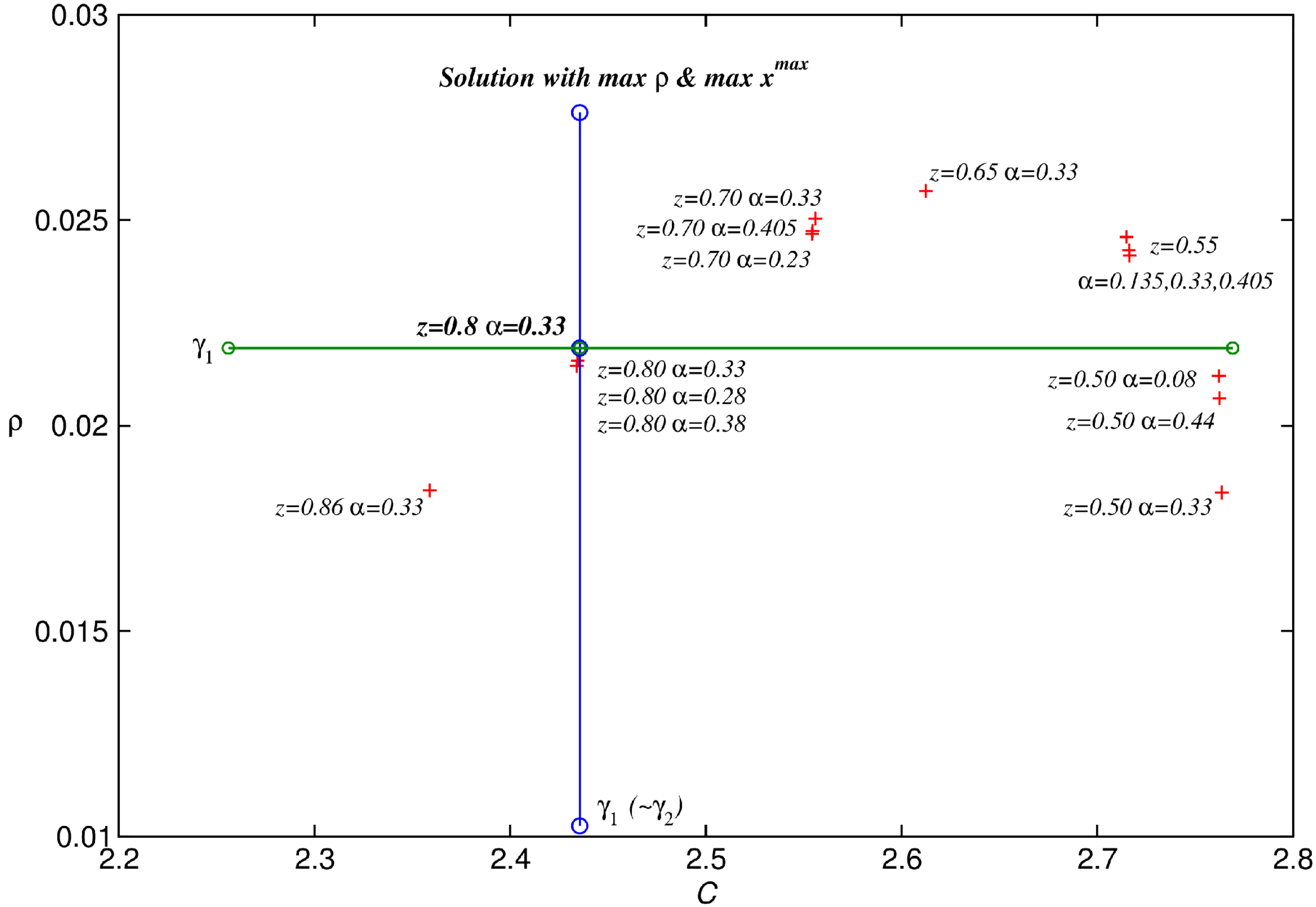

Some examples of **continuation and identification for data at the boundary, on the ZVS, with large z_0**. Note that now the **rotation number is not so small**.

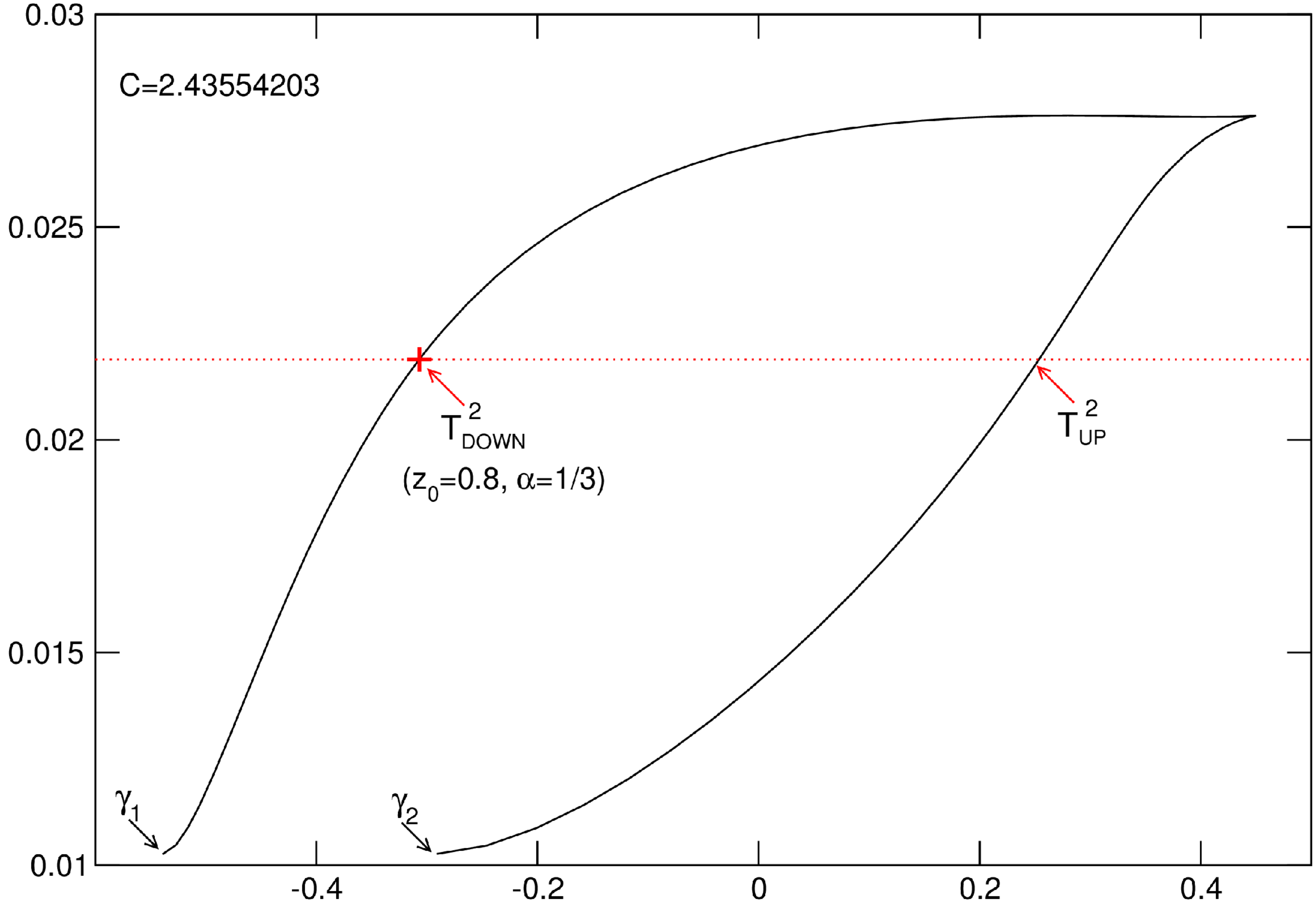

An example of **continuation for fixed C**. On the vertical axis the **rotation number** is displayed. In the horizontal one the **maximal value of x on the invariant curve**. The two lines correspond to the NHIM on the centre manifold of two periodic orbits (see later).

A problem: identification of 2D NHIM for small z_0

A **difficulty** appears when trying to **identify the NH $\mathbb{T}^2$** which **separates stable/unstable** orbits if this NH is in the **centre manifold of L_3**. We can also talk about the **invariant curve on the Poincaré section**.

Reasons:

- The **rotational dynamics under the Poincaré map is very slow**, because of the eigenvalues at L_3. At the same time the **instability is comparatively larger**. An orbit approching the NH curve **can stay close to it for very few Poincaré iterates**.
- After Leaving a vicinity of the NH curve the Poincaré iterates **move away to the left part** and return near the **centre manifold of L_3**. The number of **iterates between successive visits is of the order of hundreds**.
- Given **a level of C** and **two 2D tori on its centre manifold** they can have **heteroclinic intersections** (Arnol'd diffusion, etc). The **returns can be close to different 2D tori**.

This requires some effort to **correctly identify** the (different) 2D tori related to the escape boundary. Based on amplitude of the z component of the orbit in the suitable region.
For **large z_0** the 2D NHIM can be continuated. If the **size shrinks** they lead to a **periodic orbit**. See next slide.

A relevant family of periodic orbits

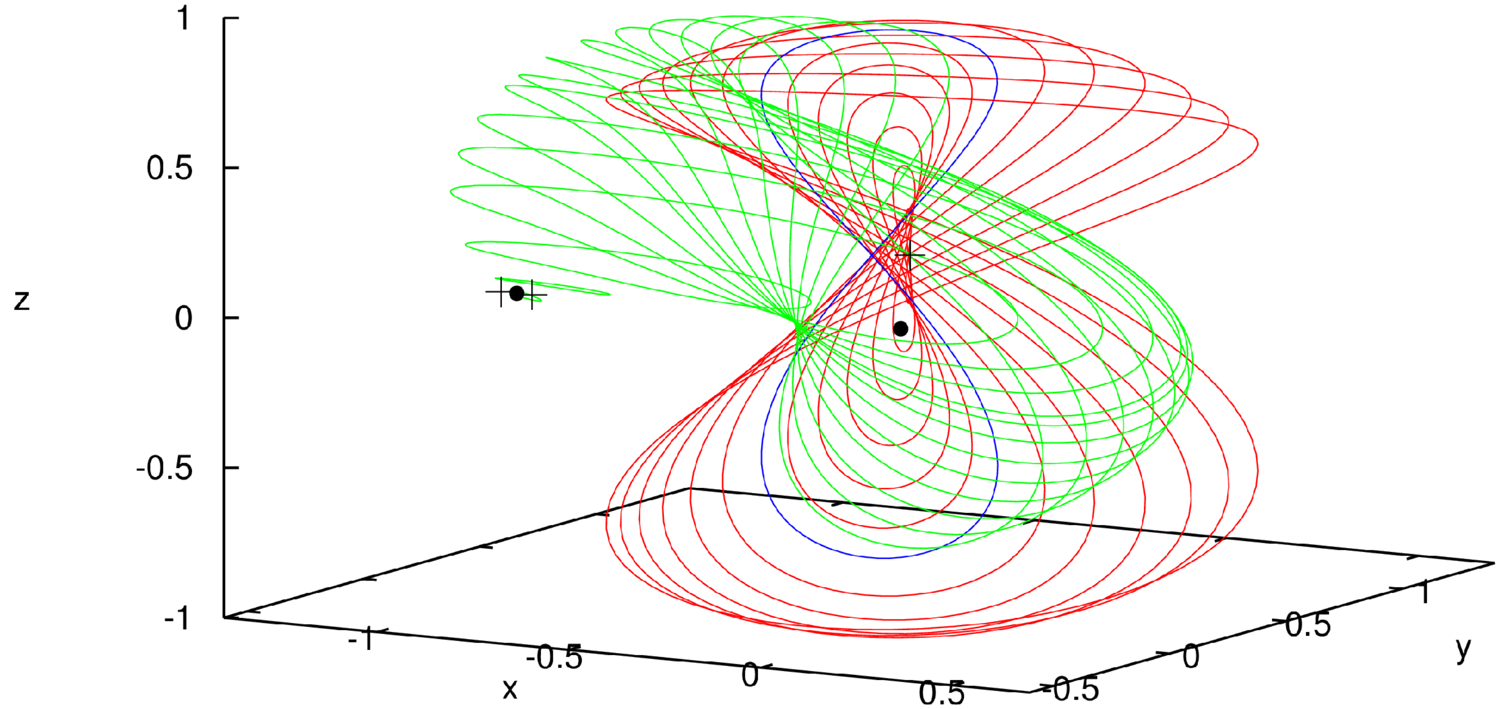

The **vertical family of Lyapunov orbits emanating from** L_4 (in blue) **bifurcates to two p.o. of saddle-centre type** (subcritically). They are **symmetric wrt to** $z = 0$. The family is a **2D object** (allowing changes in the Jacobi constant). Its **centre manifold is a 4D object**. The **stable/unstable manifolds** of the centre manifold are **5D**. They are **close to double heteroclinic connection** (small splitting), specially for large z.

Starting outside the ZVS

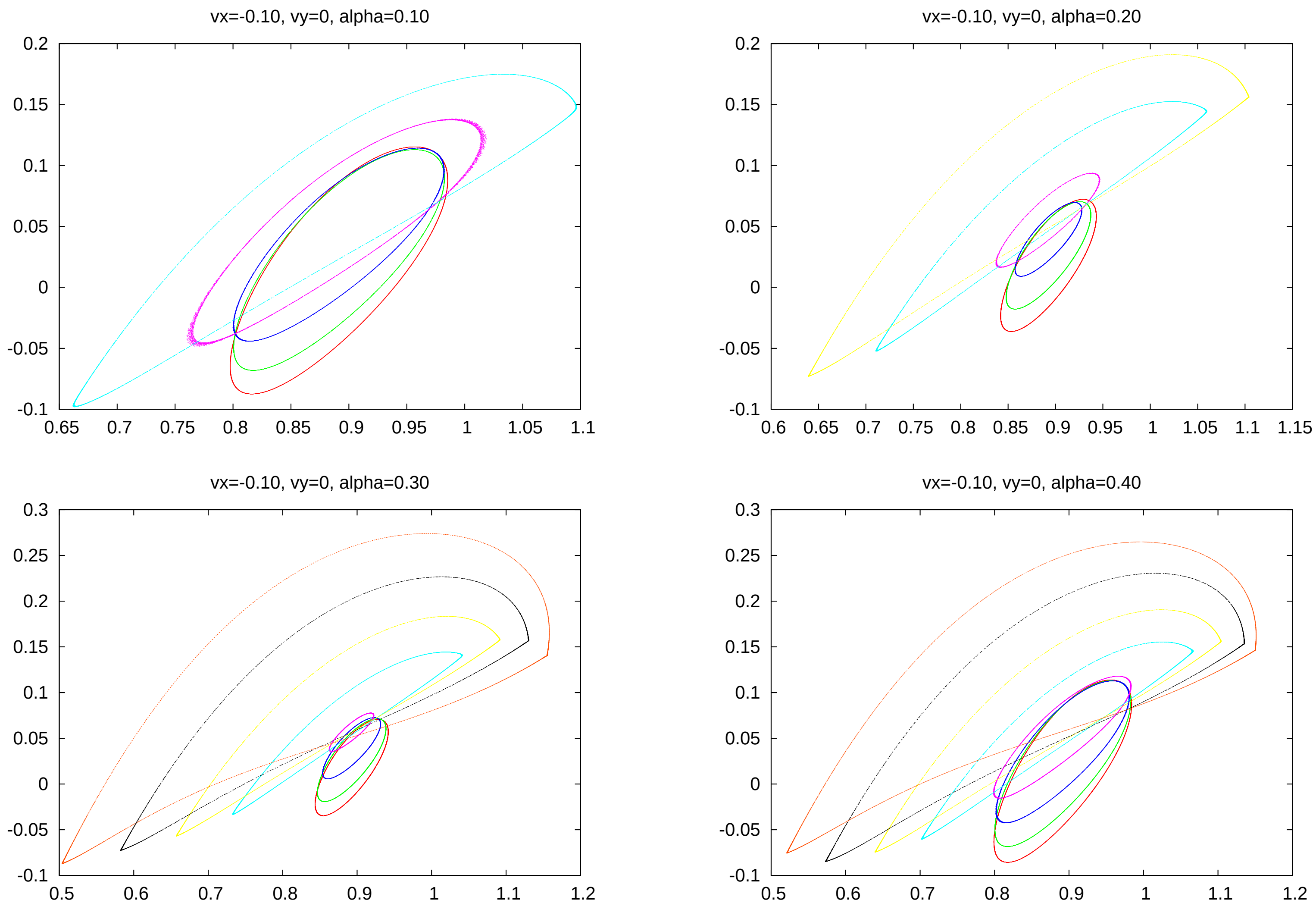

Quite similar to the initial data in the ZVS. Initial data with $v_z = 0$.

Note that for some values of the initial synodical velocity it can be necessary to compute **using 2-sections for** $x = x_0,\ x_0 \neq -0.5$. See next plots for $v_x = -0.36, v_y = -0.35, v_z = 0$ where we use $x_0 = -0.5$.

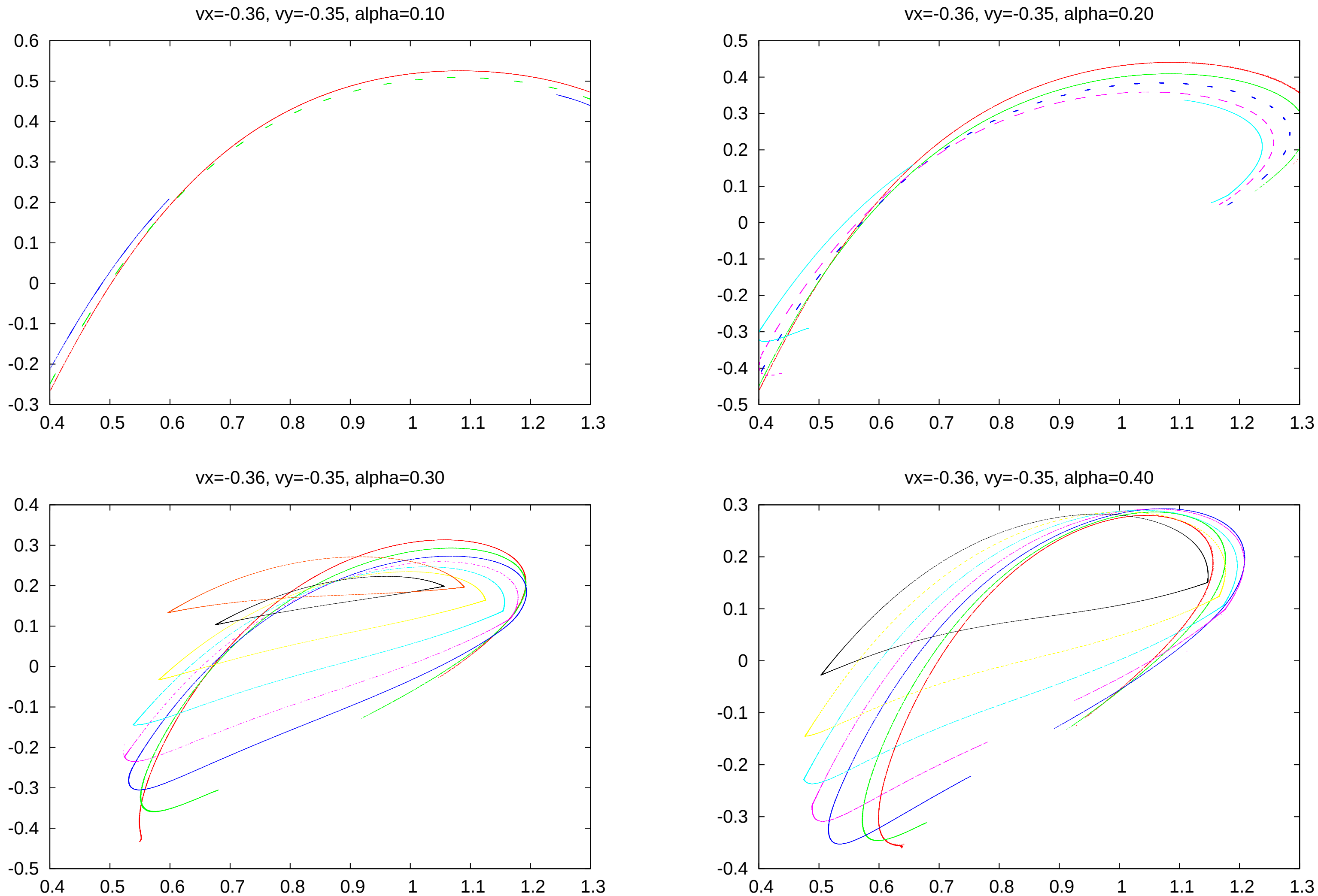

A sample of results of **2-sections for** $v_x = -0.36, v_y = -0.35$. As we use $x_0 = -0.5$ some sections are only partially seen. The colour code, as in the previous slide and in the case of the slide for data in the ZVS for $z_0 = 0.1,\ 0.2,\ \ldots 0.8$ follows the gnuplot code (red, green, blue, etc). For $\alpha = 0.1$ the z_0 goes **only up to 0.3**; for $\alpha = 0.2,\ 0.3,\ 0.4$ **up to** $z_0 = 0.5,\ 0.8,\ 0.7$, respectively.

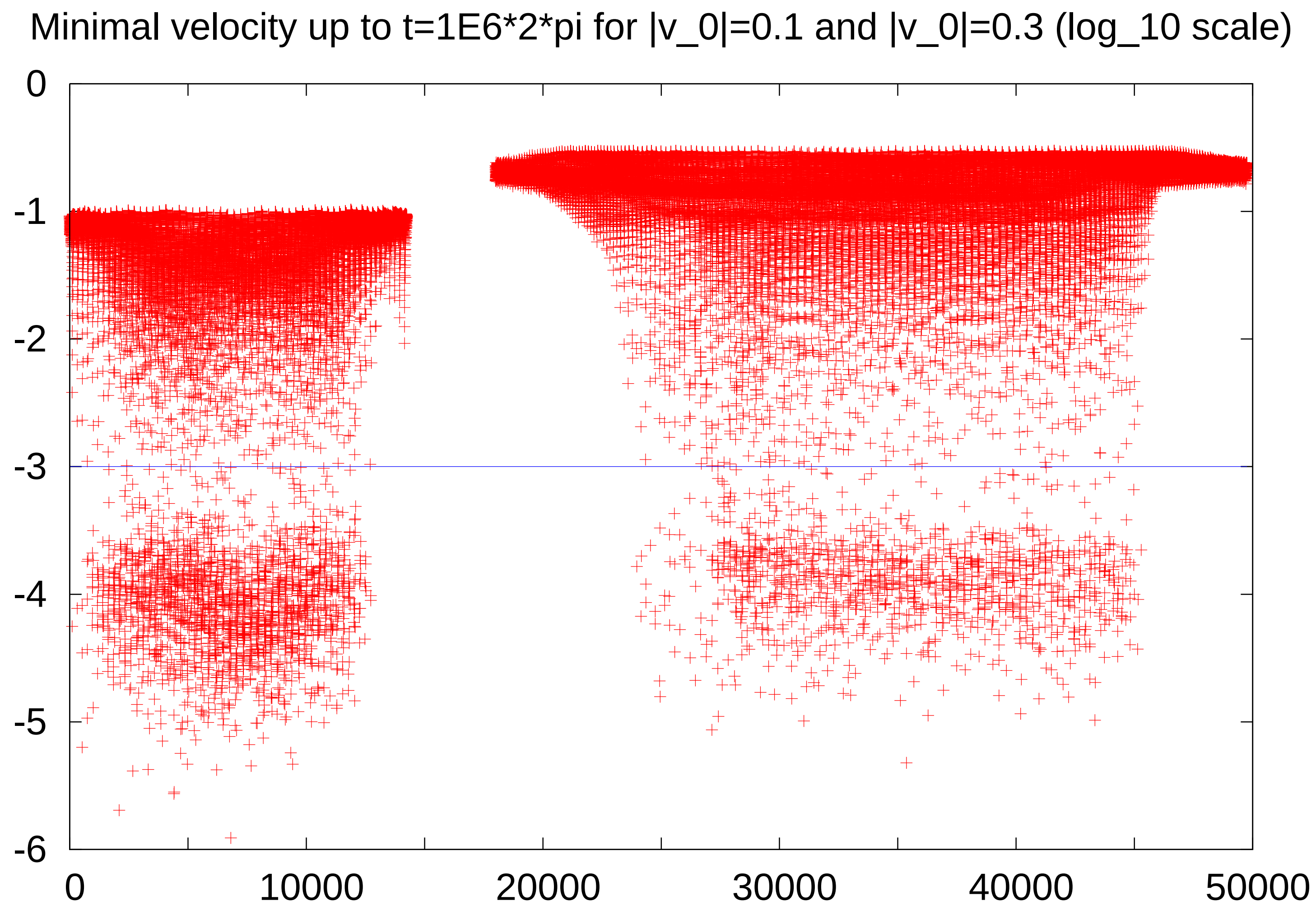

Take also into account: **many initial conditions, for different** $z, \alpha, \rho, v_x, v_y, v_z = 0$ **lead to the same torus**. Different data correspond to **different** z_0, α_0 and, from left to right, to **increasing argument of** (v_x, v_y) (from 0 to 2π).

The points below the line can be **accepted to correspond also to IC in the ZVS**. The estimate $\mathcal{O}(1/\sqrt{t})$ is in agreement with the **ergodization time**, based on **simultaneous Diophantine approximation**.

Conclusions and Outlook

- The role of some **codimension-1 manifolds** in problems of **practical stability "boundaries"** has been applied to the present problem.
- Similar tools work in other problems (some experiments did in the past) like: **elliptic 3D RTBP, bicircular coherent models**. Applications to kinetics in chemistry: **TST**. And in many other domains (**plasma physics,...**).
- These manifolds explain the **"sharp, too sharp, boundaries"** mentioned by L. Exposito in his book about **rings of planets and asteroids** (cf. talk by Lluis Benet).

As immediate work: complete computation of NHIM around L_3 and around the family of p.o. in narrow grids. Make identification cheks: (z, α, ρ) vs C and rotation number. Some additional checks with IC not in ZVS. Complete the results on splitting available right now.

Next steps:

- **perturbation methods for very small μ**,
- **Sun-Jupiter and Earth-Moon cases**,
- **NF methods around μ_2, μ_3**.

Why no Trojan-like rocks have been found in the Earth-Moon system?

Another **challenge...**.
A hint: **maybe the Sun is guilty for this...**

Poincaré revisited

In the **abstract provided by Alain Chenciner** one mentions a **sentence by Paul Appell** on the impact of **Les méthodes nouvelles de la mécanique celeste** during **next half century**. Now we know that the impact is relevant for **more than one century**.

Let me guess how the famous Poincaré sentence would read now...

The **periodic orbits are the only way to penetrate ... into the RTBP**.

Furthermore, **not only the existence is relevant**, but mainly its **stability properties**. And, in particular,

- The existence of **invariant tori** around them, of maximal or lower dimension,
- The associated **NHIM** and their **stable and unstable manifolds**,
- And the **relative positions of these manifolds**

are the only way to penetrate ... into the global description of the dynamics for Hamiltonian Systems.

Thanks for your generosity, your work and ideas, Henri